Journal Pre-proofs

Development and integration of a continuous horizontal belt filter into drug production procedure

Kornélia Tacsi, Dorián László Galata, András Domokos, Éva Pusztai, Brigitta Nagy, György Stoffán, Zsombor Kristóf Nagy, Hajnalka Pataki

PII: S0378-5173(24)00963-3
DOI: https://doi.org/10.1016/j.ijpharm.2024.124729
Reference: IJP 124729

To appear in: *International Journal of Pharmaceutics*

Received Date: 3 June 2024
Revised Date: 11 September 2024
Accepted Date: 16 September 2024

Please cite this article as: K. Tacsi, D.L. Galata, A. Domokos, E. Pusztai, B. Nagy, G. Stoffán, Z.K. Nagy, H. Pataki, Development and integration of a continuous horizontal belt filter into drug production procedure, *International Journal of Pharmaceutics* (2024), doi: https://doi.org/10.1016/j.ijpharm.2024.124729

Development and Integration of a Continuous Horizontal Belt Filter into Drug Production Procedure

Kornélia Tacsi[1], Dorián László Galata[1], András Domokos[1], Éva Pusztai[2], Brigitta Nagy[1], György Stoffán[1], Zsombor Kristóf Nagy[1], Hajnalka Pataki[1]

[1]Department of Organic Chemistry and Technology, Faculty of Chemical Technology and Biotechnology, Budapest University of Technology and Economics, Műegyetem rkp. 3., H-1111 Budapest, Hungary

[2]Department of Chemical and Environmental Process Engineering, Faculty of Chemical Technology and Biotechnology, Budapest University of Technology and Economics, Műegyetem rkp. 3, H-1111 Budapest, Hungary

KEYWORDS: Continuous filtration, Horizontal belt filter, Mixed suspension mixed product removal, Plug flow crystallizer, Acetylsalicylic acid, Design of experiments

ABSTRACT

In the pharmaceutical industry, filtration is traditionally carried out in batch mode. However, with the spread of continuous technologies, there is an increasing demand for robust continuous filtration strategies suitable for processing suspensions produced in continuous crystallizers. Accordingly, this study aimed to investigate a lab-scale horizontal conveyor belt filtration approach for pharmaceutical separation purposes for the first time. The newly developed continuous horizontal belt filter (CHBF) was tested under different systems (microcrystalline cellulose (MCC)/water, lactose/ethanol and acetylsalicylic acid (ASA)/water) and diverse conditions. Filtration was robust using a well-defined unimodal particle size distribution MCC in water system, where the residual moisture content varied within narrow limits of 45-52% independently from the process conditions. Besides, the residual moisture content highly depended on the applied solvent and particle size. It could be reduced to below 2% by processing the suspensions of either a volatile solvent (lactose in ethanol) or an aqueous slurry of a large particle size ASA. Finally, the CHBF was connected to a mixed suspension mixed product removal (MSMPR) or a plug flow crystallizer (PFC). The residual moisture content of the CHBF-filtered ASA product and operation characteristics (onset of steady-state) were evaluated in both continuous crystallizer-filter systems. The MSMPR-CHBF system operated with a longer startup period. The size of the in situ-produced crystals was of a similar order magnitude in both systems, resulting in a similar residual moisture content (around 20%). Overall, the tested continuous filter was robust, did not modify the crystal morphology in the examined experimental range, and could be effectively integrated with continuous crystallizers.

1. Introduction

Presently, batch processes are dominant in the pharmaceutical industry as, in addition to the strict authority regulations, the complexity of pharmaceutical manufacturing slows down the spread of novel

continuous technologies. Recognizing the benefits of continuous operations, strong authority and industrial incentive unfolds to transition batch processes to continuous alternatives [1,2]. Consequently, continuous technologies have become a focus of industrial and academic research and development for many years.

For solid-liquid separation, discontinuous pressure Nutsche filters and centrifuges are widespread in the pharmaceutical manufacturing environment, and most continuous crystallization technologies are followed by batch-mode filtration. At the same time, a robust and flexible continuous filtration operating in a steady-state can be effectively integrated between the continuous crystallization and the formulation procedures. There are several semi-continuous and continuous filters operating on numerous different principles, capacities, and areas of use, but only a few have been discussed in the literature for pharmaceutical purposes.

Many filters were tested in standalone mode, while a few studies addressed integrated systems. The filters typically connected with continuous crystallizers such as mixed suspension mixed product removal (MSMPR) crystallizers [32,33] or tubular crystallizers [34,35], like plug flow crystallizers (PFC) [34] and segmented flow crystallizers (SFC) [36]. Among the above, only the literature of the most relevant semi-continuous, continuous filters will be presented in detail and compared based on filtration efficacy of crystalline active pharmaceutical ingredients or additives (Table 1).

Table 1 Summary of Continuous Filtration Technologies Comparing Particle Characteristics (size, shape), Achieved Residual Moisture Content, and Important Conclusions. (abbreviations: φ: residual moisture content*, CL: cord length; SASR: solvent to antisolvent ratio, SA: standalone, C: connected crystallizer-filter system, PCM: paracetamol, BA: benzoic acid, EtOAc: Ethyl acetate, AcOH: Acetic acid, PSD: particle size distribution, SFC: segmented flow crystallizer, wow: without washing, ww: with washing, wd: with drying)

Reference	System	Suspension details (particle size, shape)	φ* [%]	Highlights
Acevedo [16]	MSMSPR & CFC	PCM/ethanol (CL: 70-80 µm, prismatic)	C: 22	Filtration did not affect morphology
		BA/ethanol/water, SASR 0.43 (CL: 110 µm, plate and needle-like)	C: 45	Crystals clustered together, liquid entrapment effect.
Liu [18]	OBR & CFC, washing with ethanol	PCM/ethanol (D50: 100-170 µm)	SA:5 C: <10	Longer washing slightly increase φ in case of lower vacuum time.
		BA/ethanol/water, SASR 0.23 (D50: 30-35 µm)	SA:15-35 C: 55	Heavy agglomeration, washing reduce φ and aid in avoiding filter medium clogging.

Domokos [19]	MSMPR & CFC	ASA solution with EtOAc, AcOH, etc./heptane. SASR: 0.5 (D43. 400-600 µm)	C: 1-6	φ was constant in the startup phase, no correlation between PSD and φ
Ottoboni [17]	CFC (SA)	PCM/ethanol Washing #1: 1/1 ethanol/heptane Washing #2: heptane	SA: 12.1	Semicontinous results are not in accordance with the predictions based on batch mode experiments.
Steenweg [21,22,24]	• CVSF (SA) • Washing 1st-stage: 4/1 ethanol/water 2nd-stage: ethanol • Drying	L-alanine/water (D_v50: 570 µm, 355−560 µm sieve fraction, octahedral, bipyramid (BP), cuboid (Cub) or needles (N))	BP: 22 (wow) BP: 1-15 (ww) Cub: 25-35 (ww) N: 11-19 (ww) Cub, N: <1 (wd)	Filtration was robust; degradation, agglomeration did not occur One-stage washing can increase agglomeration, two-stage washing with volatile solvent enables almost dry product φ shows a high dependency on particle shape; washing is not so effective. Drying module is required.
Steenweg [23]	SFC & CVSF Two-stage washing	L-alanine/water (D50: 400-500 µm, octahedral, agglomerates)	2 (ww)	Large SFC-produced particles could effectively be dried by applying two-stage washing (ethanol, water)
Wu [13]	Continuous rotary filter	API (D_v50: 400 µm, D_v90: 700 µm, rod-shaped)	C: 5.5-6.5	Washing effectively reduces impurity content
Dobler [28]	QCFBC	sucrose/water (median size: 100 µm)	C: 9	Crystal size was unaltered during filtration.

*Residual moisture content refers to the amount of moisture remaining in a material after filtration.

Alconbury Weston Ltd. patented a continuous filtration carousel (CFC), which integrates automated batch filtration, washing and drying units [14,15,17]. It consists of a rotating carousel with cylindrical chambers that can rotate to different positions to perform different subprocesses (filtration, washing, drying, discharge) separately. The concept of this filter is based on batch-wise filtration, featuring

narrow residence time distribution (RTD) coupled with easy material traceability. The pore size of the filter medium is 10 μm.

Acevedo and co-workers connected the CFC device with an MSMPR crystallizer. They found that the 70-80 μm cord length prismatic paracetamol (PCM) crystals in ethanolic suspension can be filtered with 22% moisture content. In contrast, 110 μm cord length plate and needle-like benzoic acid (BA) product in ethanol/water contained 45% moisture after filtration [16]. In the case of PCM, the morphology did not alter during filtration, while BA crystals tended to clog the filter medium; thus, cleaning the CFC with the clean-in-place method is required periodically. Liu et al. coupled an oscillatory baffle reactor (OBR) to the CFC and investigated the effect of washing with the same model slurries (PCM/ethanol and BA/ethanol/water) [18]. By filtering PCM, the residual moisture content could reduce to 5-10%, and washing with ethanol tends to increase the moisture content slightly. The washing caused larger medium-sized products as the ethanol washing solvent could dissolve fine particles. Processing the slurry of the small crystal-sized BA the φ was high, due to the presence of water. Washing with ethanol could significantly improve the filtration efficacy. The residual solvent content was higher in both connected systems than in the standalone operation. Domokos et al. used CFC to filter the multicomponent slurry of acetylsalicylic acid (ASA) produced continuously in an MSMPR crystallizer [19]. Presumably, due to the high crystal size and low scale of the filtration process, the filtration could operate with high efficiency (1-5%) independently of the product size.

The researchers of TU Dortmund patented a continuous vacuum screw filter (CVSF) which is a modular screw conveyor equipment that enables small-scale continuous isolation, washing, and drying [20–24]. A rotating polytetrafluoroethylene (PTFE) screw, placed in a tubular inner body, facilitates the axial transport of the process medium. The lower half of the inner jacket is a porous filter frit (pore size 40-100 μm) for the withdrawal of the liquid phase. Steenweg et al. found that L-alanine/water slurry can be filtered with 20-25% residual moisture, which is independent of the process parameter (suspension flow rate, solid content, rotation screw speed) [24]. Single-stage washing with ethanol/water could decrease the φ to 5.5% but also increase the agglomeration degree; a second-stage washing with ethanol eliminates agglomeration and enables 1% of φ [21]. Further study also integrated the CVSF with a slug flow crystallizer (SFC) [23]. The crystallization-induced clogging of the CVSF was avoided by implementing a heater before filtration to reach saturation temperature and eliminate the remaining supersaturation of the system leaving the SFC. The CVSF was challenged with cuboid and needle-shaped particles, where 11.6% and 24.9% φ could be reached even with two-stage washing [22]. Applying a drying module could further improve the φ, but it could also initiate the abrasion, breakage, and agglomeration of the particles.

Mascia and colleagues implemented an integrated continuous manufacturing (ICM) pilot plant and connected the MSMPR crystallizer with a continuous rotary plate filter [8–13]. Washing with a volatile solvent (isopropyl alcohol) eliminates the effect of process parameters; thus, the filter cake contained 5.5-6.6% residual moisture in all cases. At the same time, 99.9% of the impurities could be purged.

Another effective alternative for fully continuous filtration could be a vacuum belt filter in which a vacuum-driven filtration performed on a horizontally running perforated conveyor belt serves as the filter medium [37,38]. This technology separates solids from suspensions in mining, food, or chemical industry [39] and is only rarely used to process drug substances [39]. Huttunen et al. used a soft sensor to determine the real-time moisture content of the product based on temperature change information [40]. Although some equipment manufacturers offer high-scale vacuum belt filter devices for the pharmaceutical industry [41,42]; the application of these systems in pharma R&D is underrepresented in the literature, potentially because the capacity of commercially available vacuum belt filters (85 kg/h) exceeds the capacity required for drug R&D. Based on vacuum belt filtration concept, a quasi-continuous filter belt crystallizer (QCFBC) was developed by a research team from TU Dortmund [25–31]. This modular device incorporates containers that move on a belt (mesh size 22 μm) through different stages of the production line, starting from crystallization to final product drying. Using the pilot scale QCFBC, Dobler et al. managed to crystallize 100 μm sucrose from water and reduce the moisture content of the product from 29% to 9% [28]. As the various technological steps take place on

the same conveyor belt, the residence time (RT) for each step is fixed and uniform, making the technology less flexible in this regard. Consequently, it typically operates with a long filtration time.

Evaluating the literature, CFC was effectively connected with tank crystallizers (MSMPR, OBR) operating with relatively low productivity (0.1-1 g solid/min) and featuring intermittent product removal. Its integration with technologies operating with continuous product removal (overflow MSMPR, PFC) requires a buffer tank and extra pump capacity. Fouling issues in CFC were avoided by clean-in-place (CIP) periodic washing with a good solvent of the filtered solids; however, these washing procedures could interrupt steady-state operation. The filtration efficacy of CVSF is compelling; however, due to the relatively large pore size, only slurries of well-filterable, large-sized crystal fractions could be filtered. Nevertheless, the filtration of difficult-to-filter particles was less efficient and must complemented with drying. Volatile solvents (ethanol, ethyl acetate) could be removed efficiently (<10%), while the filtration of aqueous slurries was established with high φ. Introducing volatile solvent as a washing agent effectively reduced the φ during washing (<2%) in each system.

Investigating novel lab-scale filtration strategies and integrating them with continuous crystallization technologies could be a valuable step toward implementing the connection of continuous technologies in R&D or low-capacity drug manufacturing. In order to fill the gaps identified during the literature review, specifically the lack of a lab-scale continuous vacuum belt filter in pharmaceutical applications, the aim of this study is twofold:

(i) Evaluation of the filtration efficiency of a newly developed lab-scale continuous horizontal belt filter (CHBF) by testing the parameter dependence of the residual moisture content with MCC/water and ASA/water systems. This study investigated the effects of suspension characteristics (solid concentration, solid particle size) and process parameters (mass flow rate, process time). Additional experiments were conducted to examine the solvent effect using a lactose/ethanol system.

(ii) Integration of continuous crystallizers (MSMPR crystallizer and PFC) with the lab-scale vacuum belt filter to reveal the influence of ASA crystallization parameters (crystal size, solvent content) on filtration efficacy and study the washing in the integrated PFC-CHBF system.

2. Materials and methods

2.1 Materials

For the experimentation, microcrystalline cellulose (MCC, Vivapur® 200, JRS Pharma, Rosenberg, Germany), lactose monohydrate (GranuLac® 70, Meggle, Germany), acetylsalicylic acid (ASA, >99.0%, Sigma-Aldrich, USA), and salicylic acid (SA, >99.0%, Sigma-Aldrich, USA) were used. The applied solvents were purified tap water (prepared in the lab) and ethanol (99.8%, Reanal).

2.2 Continuous horizontal belt filter characterization

The continuous horizontal belt filter (CHBF) was designed and manufactured by H-ION Ltd. (Hungary). The CHBF enables fully continuous operation. The SEFAR TETEX® DLW Classic 05-8000-C-007 type filter belt (material: polypropylene (PP), pore size: 7 µm, belt width: 200 mm, total belt length: 2800 mm, thickness: 820 µm, Sefar AG, Switzerland) was used as a filter media. A continuously running endless horizontal belt was prepared from this filter belt by slant welding (45° with 40 mm longitudinal overlap). The filtration was carried out in a process field bordered by a trough placed above the filter belt. The process field parameters are 57 mm wide, 1020 mm long, and 581.4 cm^2 filter area. Images illustrating CHBF are presented in Fig. 1 and Fig. 2.

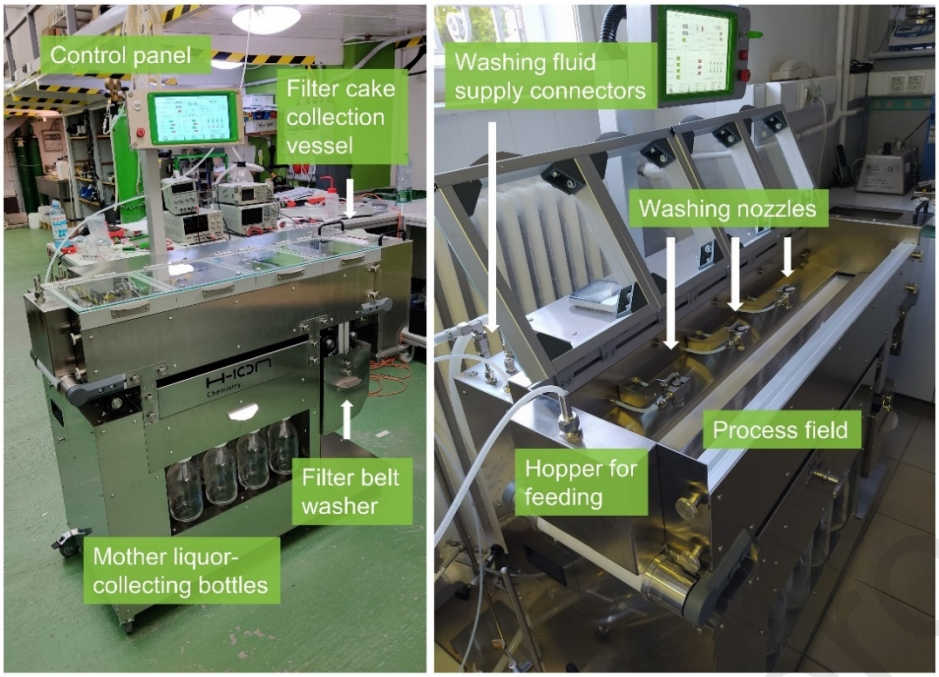

Fig. 1 Pictures of the CHBF setup.

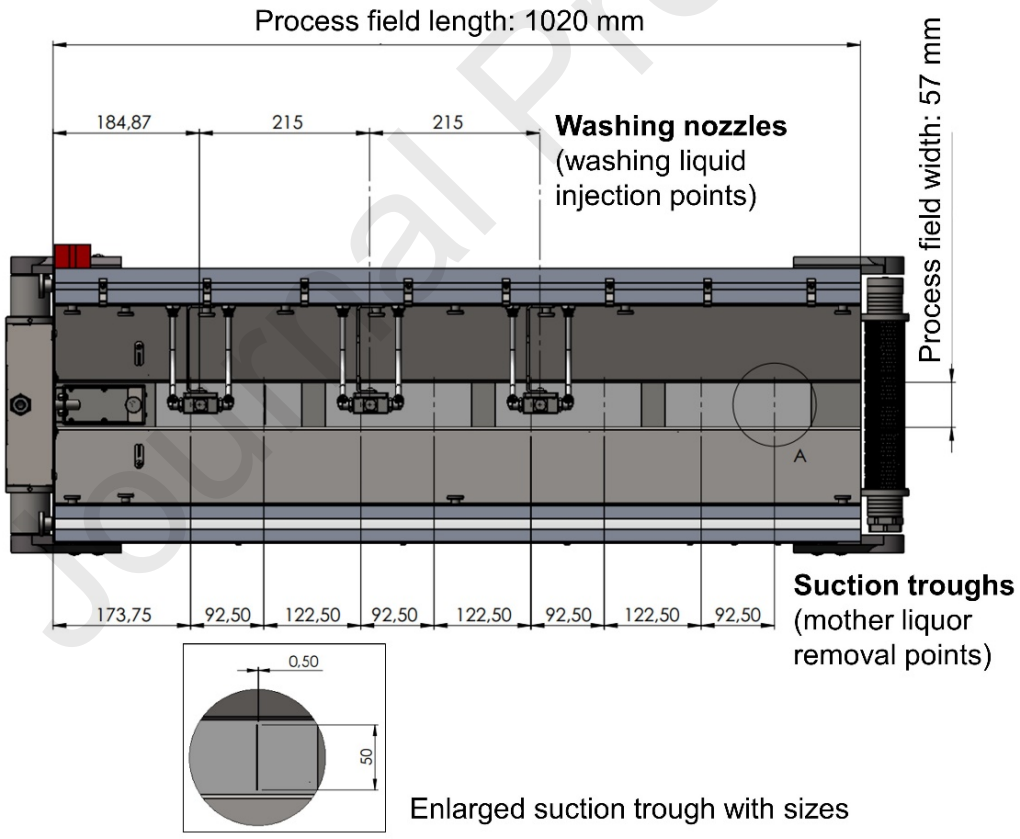

Fig. 2 Schematic top view image of the CHBF process field.

The removal of mother liquor takes place in four vacuum zones. One vacuum zone included two suction troughs, and the parameters of these troughs were the following: width: 50 mm, length 0.5 mm, and 25 mm^2 each. The vacuum zones can be turned on and off individually. All vacuum zones were active during the experiments. A ME 16 NT Diaphragm pump (VACUUBRAND, Germany, pumping speed: 16.4 m^3/h, ultimate vacuum: 70 mbar) was used for the vacuum supply. The removed filtrate is drawn into the Duran® pressure plus+ 1000 mL borosilicate glass bottles. Two vacuum-resistant bottles belong to each vacuum zone and have been filled alternately. Level sensors indicate when the bottles are filled with mother liquor. Upon receiving a signal from the level sensor, the system automatically initiates the filtrate collection in the other bottle. Operators subsequently remove the mother liquor from the filled bottle.

The filtration process is illustrated in Fig. 3. The residual moisture content is evenly distributed within the cake and can form liquid bridges between the particles. The amount of trapped fluid can be significantly affected by the porosity of the particles.

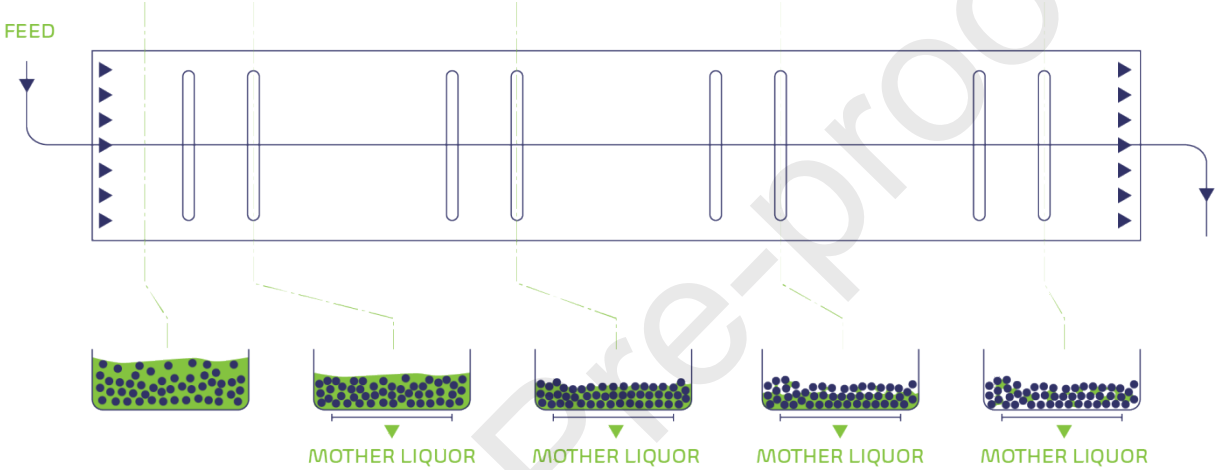

Fig. 3 Schematic top view image of the CHBF process field illustrating the filtration process along the filter belt.

The CHBF was equipped with a washer system containing three separate two-way pneumatic washing nozzles. The washing liquid was entered via an SUL 1640 B31 type atomizer (PNR Italia, Italy), producing a wide-angle full cone spray. Compressed air is introduced in washing nozzles to create the appropriate washing liquid jet. The washing liquid was dosed using a Hei-FLOW Value 01 Multi multi-channel peristaltic pump (Heidolph Instruments, Germany). The washing nozzles can be individually switched, allowing for customization of the quality and quantity of the washing liquid for each zone. Using the washer system without washing liquid can also perform a drying function by introducing only compressed air through the washing nozzles.

Based on the preparation method, we used two types of suspensions. (i) In the standalone CHBF system, a manually prepared, homogeneous suspension was fed. (ii) In the integrated systems, suspension produced in a continuous crystallizer (either MSMPR or PFC) and continuously leaving the crystallizer was dosed into the filter. Peristaltic pumps delivered all feed slurries continuously with a constant flow rate. Watson-Marlow 120U and Sci-Q 323 (UK) single-channel peristaltic pumps were used for feeding.

The suspension was transferred to the filter medium through a hopper. It was spread over the filter cloth, which moved at a constant speed. At the end of the filter surface, the crystals were removed by a scraper and fell into the filter cake collection vessel. The process time determines the period the solid material spends on the belt from feeding to removal. It could be set between 200-1000 sec. It is not equivalent to filtration time since filtering occurs in the filter zones and not along the length of the entire conveyor belt. After removing the filtered solids from the belt, the filter medium was continuously regenerated by washing the belt with a water jet of the same width as the filter surface.

In each experimental setup, parallel samples were collected at the end of the filtration. To obtain the residual moisture content of the samples, the samples were weighed after filtration and dried until reaching constant weight using a Vaciotem-T vacuum dry oven (J.P. Selecta, Spain). The MCC and lactose were dried at 105°C, while ASA was dried at room temperature to avoid its thermal decomposition while water leaves. The residual moisture (φ, %) content was calculated with the following formula:

$$\varphi = \frac{m_W - m_D}{m_W} \times 100 \quad (1)$$

where m_W is the weight of the wet sample and m_D is the weight of the dried sample.

2.3 Experimental methods

2.3.1 Experiments with the standalone CHBF

2.3.1.1 Filtration of MCC/water

An experimental series with MCC in water was performed to reveal the solid concentration, mass flow rate of the suspension and filtration time (process time) dependence of residual moisture content of the filtered product. The set levels of the process parameters are summarized in Table 2.

Table 2 Levels of Investigated Parameters during Filtration of MCC/Water Slurry in Standalone CHBF

	Lower (–)	Center (0)	Upper (+)
Solid concentration (g solid/kg solvent)	20	40	60
Mass flow rate (g solution/min)	30	40	50
Process time (sec)	200	600	1000

Further continuous experiment was carried out to study the maximum loading of the CHBF. A 176.5 g/kg MCC/water suspension was fed into the conveyor belt with an increased mass flow rate (70-136 g/min).

2.3.1.2 Filtration of lactose/ethanol

An ethanolic slurry of lactose with a solid concentration of 150 g/kg was prepared to test the CHBF with a volatile solvent. The filtration efficacy was investigated using mass flow rates of 28.3 or 81.3 g/min and process times of 200 or 1000 seconds.

2.3.1.3 Filtration of ASA/water

The filtration efficacy of the standalone CHBF was also tested with the suspensions of the commercially available, large crystal-sized ASA/water and of the small-sized ASA/water. The latter was produced previously in an ultrasonicated plug flow crystallizer (PFC) [43]. The suspensions were prepared by mixing saturated ASA aqueous solutions (0.0042 g ASA/g water at 25°C, based on [44]) and an appropriate amount of solid ASA.

The same 2-by-2 factorial design was carried out for both ASA suspensions following the Design of Experiment (DoE) methodology. In each experiment, the mass flow rate was kept constant at 40 g/min. While the solid concentration and process time parameters were similar to those applied in the MCC/water system (see Table 3). Two or three parallel center-point experiments were performed to assess the reproducibility and repeatability of results within the experimental region. Multiple samples were collected for each parameter combination to study the variability of moisture content under the same conditions.

Table 3 Levels of Investigated Parameters during Filtration of ASA/Water Slurry in Standalone CHBF

	Lower (–)	Center (0)	Upper (+)
Solid concentration (g solid/kg solvent)	20	40	60
Process time (sec)	200	600	1000

2.3.2 Experiments with the integrated crystallizer-CHBF systems

2.3.2.1 Experimental setup of integrated MSMPR crystallizer-CHBF system

Fig. 4 illustrates the schematic image of the MSMPR-CHBF system. Accordingly, the CHBF was fed directly with a suspension produced in a continuous MSMPR crystallizer. The MSMPR crystallizer was an 86 mL volume jacketed glass reactor equipped with an overflow tube. This crystallizer was utilized in previous research by the authors [45]. The suspension was agitated using a DLAB magnetic stirrer and a 4 cm magnetic stir bar. The temperature of the MSMPR crystallizer was set to 25°C using a monofluid thermostat (Huber Ministat 230). The temperature of the stirred suspension was measured with a Pt-100 thermometer. The ethanolic solution of ASA (ASA concentration was 160 mg/mL or 0.24 g ASA/g solvent) and antisolvent (purified water) was fed continuously with Watson-Marlow 120U and Sci-Q 323 (UK) single channel peristaltic pumps to the MSMPR crystallizer. The sum of the ASA solution and antisolvent volume flow rates was 32 mL/min, thus, the RT in the MSMPR crystallizer was 2.67 min. The SASR was set to 0.5. The produced ASA suspension was withdrawn continuously through the overflow tubing by the speed of feeding and it was fed directly to the CHBF. The mass flow rate of slurry exited from the MSMPR crystallizer was 37.7 g/min. The process time of CHBF was set to 200, 600, or 1000 sec.

To gain information from the crystallization process, we have collected a few samples directly from the crystallizer onto G2 or G3 glass filters and filtered batch-wise using an MZ 2C diaphragm vacuum pump (VACUUBRAND, Germany, pumping speed: 1.9/2.1 m3/h, ultimate vacuum: 9 mbar). The crystals yielded directly from the MSMPR crystallizer or the CHBF were characterized by crystal size, CSD, crystal habit (Section 2.4.2), and moisture content (φ, %).

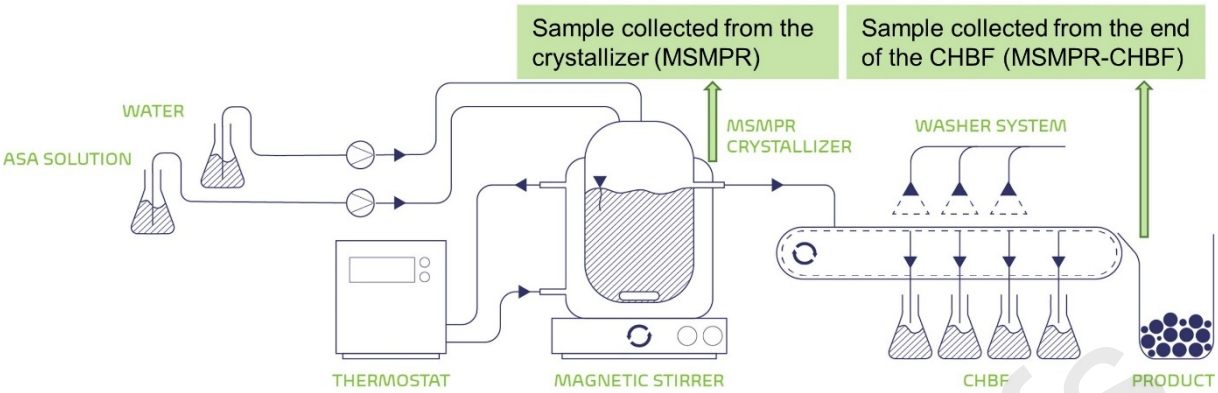

Fig. 4 Schematic image of the integrated MSMPR-CHBF system, indicating sampling locations.

2.3.2.2 Experimental setup of the integrated PFC-CHBF system

The schematic image of the integrated PFC-CHBF system is presented in Fig. 5. The ASA suspension was produced in an ultrasonicated PFC that was recently published by the authors [50]. The ASA solution and the antisolvent were mixed in a coaxial mixer connected to polytetrafluoroethylene (PTFE) tubing (inner diameter: 2 mm, outer diameter: 3 mm). The entire tubing was placed in a Bandelin Sonorex RK 510 type ultrasonic bath (ultrasonic peak power: 640 W, ultrasonic nominal power: 160 W) to provide intense agitation and avoid clogging of the crystallizer. The ethanolic solution of ASA (160 mg/mL or 0.24 g ASA/g ethanol) was fed using a Jasco PU-980 HPLC pump, while the water antisolvent was dosed with a Syrris Asia syringe pump. The SASR was 0.5. The PFC operated with 0.5 min RT while the temperature was set to 25°C. Only one sample was collected directly from PFC, as our previous experiments with PFC proved the robustness of this technology [43].

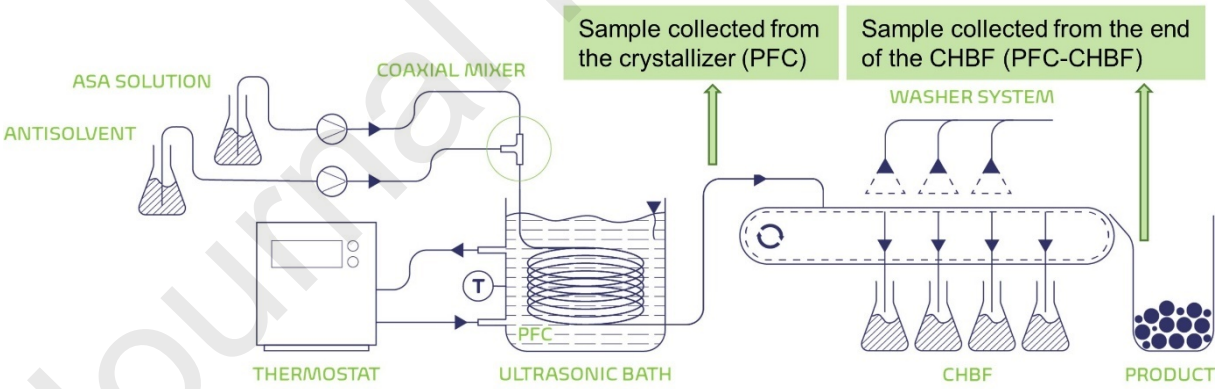

Fig. 5 Schematic image of the integrated PFC-CHBF system, indicating sampling locations.

The PFC-produced ASA suspension was filtered using the CHBF, with process times of 200, 600, and 1000 seconds. The mass flow rate of the ASA suspension was 35.5 g/min. The washing effect was studied in the connected system by analyzing the moisture and purity content. Furthermore, the RTD of the solid particles on the CHBF was measured using image analysis. More information about the RTD measurement can be found in the Supplementary Material.

Investigation of washing

In the connected PFC-CHBF system, the effect of washing on the purity and moisture content of the product was also investigated. The process parameters in the continuous crystallization were similar to condition presented above (Section 2.3.2.2). The studied washing configurations were as follows: (i) all washing zones were inactive, (ii) only the first washing zone was active, or (iii) the first and second washing zones were active. All these washing configurations were tested with process times of 600 seconds. We used water as washing liquid, dosed with a 19.6 mL/min flow rate. The SA impurity content of the collected samples was analyzed with HPLC, according to the method described in Section 2.4.1.

2.4 Characterization of the product quality

2.4.1 High-performance liquid chromatography (HPLC) analysis

The SA impurity content of ASA products was measured with a reverse phase HPLC (Agilent 1200 series LC System) according to the method developed by Balogh and co-workers for determining the SA to ASA ratio of crystalline samples [46]. The purity of the washed ASA samples produced in the connected PFC-CHBF system was studied. An EtOH solution with 1 mg/mL concentration was prepared from the recently filtered ASA crystals. Following this, the solutions were diluted at a 1:20 ratio using a mixture of acetonitrile, methanol, and phosphoric acid (ACN: MeOH: H3PO4 in a 92:8:0.5 v/v%) to maintain the chemical stability of ASA until the subsequent HPLC measurement [47].

HPLC measurements were conducted using a Supelco Inertsil ODS-2 C18 column (GL Sciences, Japan, 5 μm; 250 × 4.6 mm). 5 μL of the diluted sample was injected for analysis. Isocratic elution was performed using an eluent consisting of 60% ACN and 40% water−phosphoric acid mixture (200:1 ratio). The analysis lasted 5 minutes. The ASA and SA were detected with 2.1 and 2.6 minutes retention times, respectively. The impurity content in the crystalline product was calculated based on the peak area ratio.

2.4.2 Crystal habit, crystal size, and crystal size distribution characterization

The CSD of filtered crystals was analyzed offline with Malvern Mastersizer 2000 (Malvern Instruments, UK) equipped with a Scirocco 2000 dry powder feeder (Malvern Instruments, UK). We introduced around 100 mg of the solid sample into the feeder, dispersing it with an overpressure of 1 bar. The measurement lasted for 30 sec, followed by a 10-sec cleaning phase. The product CSD was evaluated with volumetric distribution values (D_v10, D_v50, and D_v90) obtained using the Malvern Mastersizer 2000 program (version 6.01). The crystal morphology of the products was observed through a CKX53 inverted microscope equipped with an 18Mp CAM-SC180 Camera set.

2.4.3 Statistical analysis

Some experimental results were evaluated using the TIBCO Statistica program (version 14.0). A significance level of 0.05 was set for the statistical analysis. The factorial design experiments were carried out in a randomized order.

3. Results and discussion

In accordance with the study aims, the filtration efficacy in the CHBF was investigated in standalone mode and by connecting the CHBF with continuous crystallizers. The examined suspensions and the aim of these experiments are outlined in Table 4.

Table 4 Overview of the Experimentally Examined Systems Regarding Operation Type and the Studied Parameters

Operation type	System	Studied parameters
Standalone	MCC/water	Solid concentration, mass flow rate, process time effect of moisture content. Tests with extra workload.
	Lactose/ethanol	Experiments in ethanol were conducted to examine filtration in a volatile solvent.
	commercial (large) ASA/water	Particle size and process time effects on residual moisture content.
	PFC-produced (small) ASA/water	
Integrated	MSMPR-CHBF	Process time dependence of residual moisture content.
	PFC- CHBF	Process time dependence of residual moisture content. RTD measurement. Test of washing.

3.1 Effects of filtration parameters on filtration efficacy

Continuous experiments were performed in the standalone CHBF with an MCC/water system to evaluate the filtration efficacy regarding the residual moisture content. MCC is a widely employed tableting excipient in the pharmaceutical industry as a filler and binder. MCC is insoluble in water and has a narrow particle size distribution, making it a suitable model component for aqueous filtration. The MCC/water suspension contained large, spherical and columnar particles featured with unimodal CSD (D_v10: 101.3 ± 1.6 µm, D_v50: 239 ± 3.6 µm, D_v90: 440.6 ± 3.6 µm). Table S1 in Supplementary Material summarizes the crystal shape, size and CSD characteristics of the MCC.

While determining the investigated experimental region, we considered the following aspects:

(i) The solid concentration ranged from 20 g/kg (1.96%) to 60 g/kg (5.66%), which is comparable to typical small molecule crystallization processes and aligns with the range studied in the relevant literature.

(ii) The mass flow rate was maintained between 30 and 50 g/min, as this allowed for the formation of a uniform filter cake that evenly covered the entire process field, while also keeping the material requirement for the experiments reasonable during longer (60-minute) operations.

(iii) The process time could be varied between 200 and 1000 seconds; therefore, these were the limit values for this factor.

According to our observations, the majority of the mother liquor was removed in the first vacuum zone regardless of the height of the filter cake. The filtration process in the CHBF was similar in each parameter setting. The moisture content results in continuous filtration, summarized in Table 5.

Table 5 Residual Moisture Content During MCC/water Filtration Carried Out in a Standalone CHBF

Solid concentration [g solid/kg solvent]	**Mass flow rate [g solution/min]**	$t_{process}$ **[sec]**	$\varphi*$ **[%]**
20	30	200	50.97
20	30	1000	45.79
20	50	200	51.54
20	50	1000	52.19
60	30	200	50.43
60	30	1000	51.43
60	50	200	52.13
60	50	1000	52.07
40	40	600	50.55
40	40	600	51.09
40	40	600	51.03

*One sample was collected in each parameter setting combination; therefore, the standard deviation values could not be reported.

It was found that regardless of the set process conditions, the φ ranged from 45.8 to 52.2%. The results revealed that the investigated process parameters had no significant effect on the φ. Based on this, filtering in the CHBF proved to be highly robust.

An additional load test was carried out to challenge the continuous filter and investigate the maximum capacity of the CHBF. For this, we prepared an MCC slurry with maximum solid concentration (176.5 g MCC/kg water suspension), which still ensures homogeneous mixing and feeding. It was dosed onto the process field at a mass flow rate of 70-136 g/min. The maximum amount of filtered solid MCC was appr. 1200 g/h, when the height of the filter cake was 15 mm, reaching the height of the outlet opening at the end of the trough. The process time was set to 1000 sec. The images about the max loading of the CHBF are presented in Fig. 6.

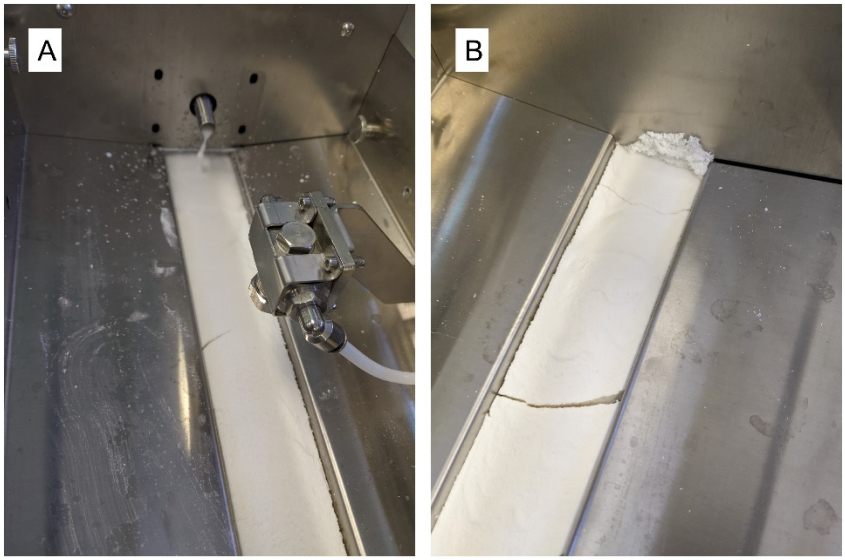

Fig. 6 Picture A and Picture B present the inlet and outlet of the CHBF, respectively, during experiments with increased workload (mass flow rate: 136 g/min).

The moisture content of the product at mass flow rates of 70 g/min and 136 g/min was 55.6 ± 2.5% and 59.7 ± 2.6%, respectively. According to our observations, most of the mother liquor was collected in the first vacuum zone, similar to the experiments with average load. The decrease in process time did not alter the residual moisture content significantly. Based on the measured moisture content and filtration process, the CHBF operation was robust in the case of significantly higher solid loading.

Overall, the filtration of this aqueous suspension can be carried out with moderate efficiency. In the case of a normal operating range regarding workload (solid concentration, mass flow rate), the filtration efficiency is not sensitive to the amount of filtered material (i.e., the cake thickness) or the process time. Therefore, it can operate with maximum efficiency even with a filtration time of 3.3 minutes. The robustness of this technology, which is proven with increased workload, can be paramount in an industrial environment.

3.2 Solvent effect on moisture content

The filtration efficacy of the CHBF was also studied with an organic solvent, namely ethanol. Lactose (GranuLac® 70, Meggle, Germany) was selected as the model ingredient as it featured low ethanol solubility. The suspension contained fine, sharp-edged cuboid particles with narrow unimodal CSD (D_v10: 21.5 ± 0.4 µm, D_v50: 131.8 ± 1.0 µm, D_v90: 258.6 ± 4.2 µm). Table S2 in Supplementary Material summarizes the crystal shape, size and CSD characteristics of the lactose. The solid concentration was set at 150 g/kg. The studied parameter combinations and the belonging moisture contents are summarized in Table 6.

Table 6 Residual Moisture Content During Lactose/ethanol Filtration Carried Out in a Standalone CHBF

	Mass flow rate [g/min]	**Process time [sec]**	***φ*** **[%]**
Lac_1	28.3	200	0.3 ± 0.0

Lac_2	28.3	1000	0.9 ± 0.3
Lac_3	81.3	200	0.5 ± 0.5
Lac_4	81.3	1000	1.4 ± 1.3

The moisture content of the CHBF-filtered lactose was below 1.4% on average at all measurement points. Almost completely dry lactose left the filter. It did not show a clear correlation with the process parameters.

In the case of the ethanol suspension, the material needed to spread evenly across the filter and form a uniform filter cake. Initial experiments were conducted using a suspension with a lower solid concentration, during which the filter cake surface was more susceptible to cracking. The appearance of cracks could result in higher moisture content in the product. Despite all these, the filtration of ethanol suspension was proved to be significantly better regarding moisture content compared to the filtration of aqueous MCC systems.

3.3 Crystal size effect on moisture content

The particle size of the crystallized product can be very different; thus, the effect of the crystal size on the filtration efficiency was investigated in the standalone CHBF. We used the ASA model ingredient, which was also used in connected continuous crystallization-filtration experiments. Premade water suspensions with PFC-produced (small-sized) and commercial (large-sized) ASA crystals were filtered. The solid phase characterization of initial ASA crystals is summarized in Table 7.

Table 7 CSD plots, D_v values, and microscopic images of the PFC-produced and the commercial ASA.

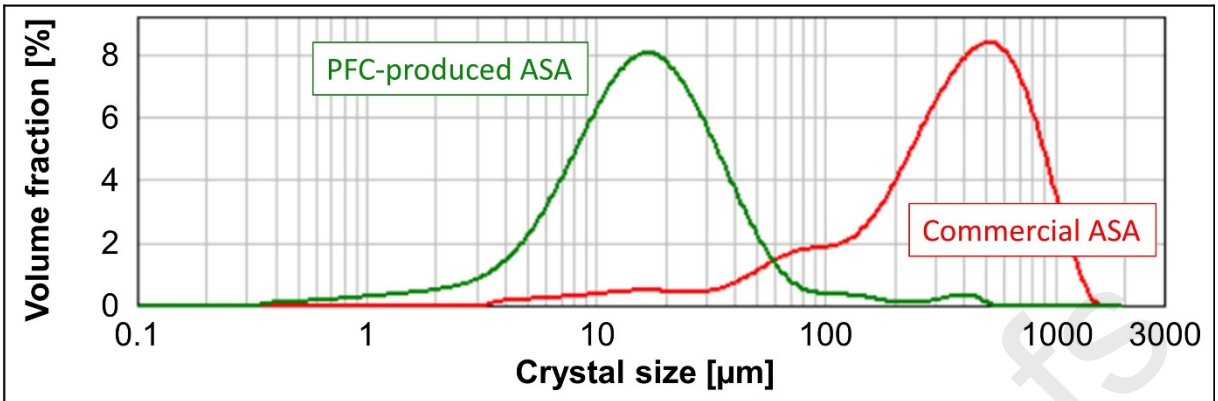

PFC-produced ASA			Commercial ASA		
D_v10 [µm]	D_v50 [µm]	D_v90 [µm]	D_v10 [µm]	D_v50 [µm]	D_v90 [µm]
5.3 ± 0.1	15.7 ± 0.5	41.9 ± 0.1	61.4 ± 7.8	383.3 ± 7.7	849.2 ± 13.9

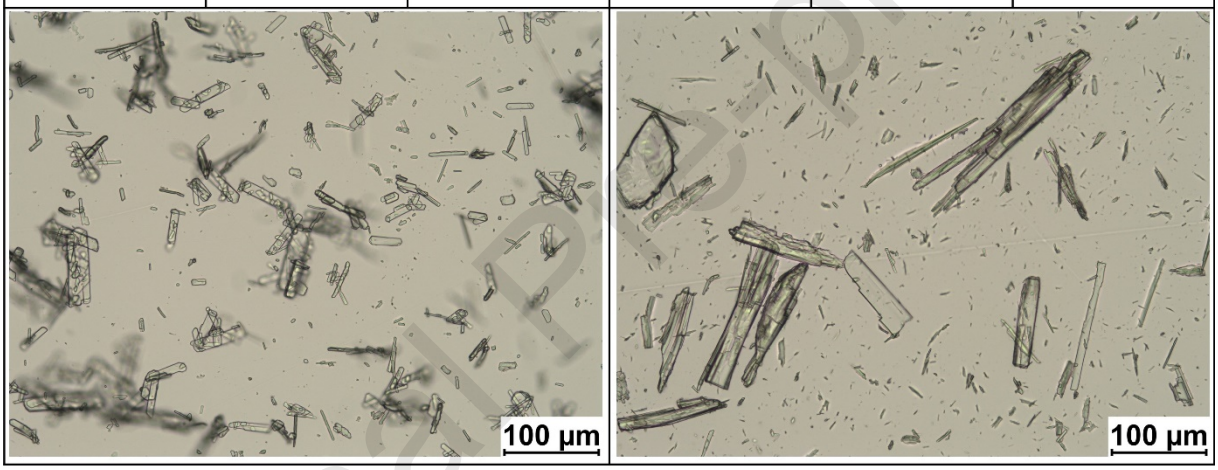

The moisture content, as a function of the applied filtration process parameters, is summarized in Table 8.

Table 8 Residual Moisture Content During Filtration of ASA/water Slurries Carried Out in a Standalone CHBF

Solid concentration [g solid/kg solvent]	$t_{process}$ **[sec]**	φ **[%]**	
		PFC-produced (small-sized) ASA/water	**Commercial (large-sized) ASA/water**
20	200	43.3 ± 0.6	1.9 ± 0.4
20	1000	43.7 ± 9.6	0.3 ± 0.1

60	200	53.8 ± 1.4	1.2 ± 0.7
60	1000	49.5 ± 1.4	0.2 ± 0.1
40	600	53.7 ± 0.7	0.7 ± 0.1
40	600	54.6 ± 6.0	0.5 ± 0.0
40	600	51.2 ± 4.4	-

The φ in small-sized PFC products varied between 37% and 55%, while large-sized commercial ASA was managed to dry almost entirely (max 2%) at the end of the filtration process. In conclusion, a significantly higher residual moisture content was measured by decreasing the particle size. This is also consistent with the literature, which states that smaller crystals could be filtered less effectively from water due to higher specific surface area, as more moisture could remain in larger surface areas. The results of small-sized ASA are comparable to those experienced with the MCC/water system; however, in the case of 40 μm ASA crystals, the moisture content fluctuated in a broader range by modifying the filtration parameters.

Statistical analysis was also performed to reveal the effect of filtration process parameters on moisture content. The solid concentration and process time were set according to the rules of DoE. Orthogonal 2 by 2 factorial designs were performed in both cases. Due to the repeated center-point experiments, the repeatability of the process and the linearity of the fitted model were evaluated.

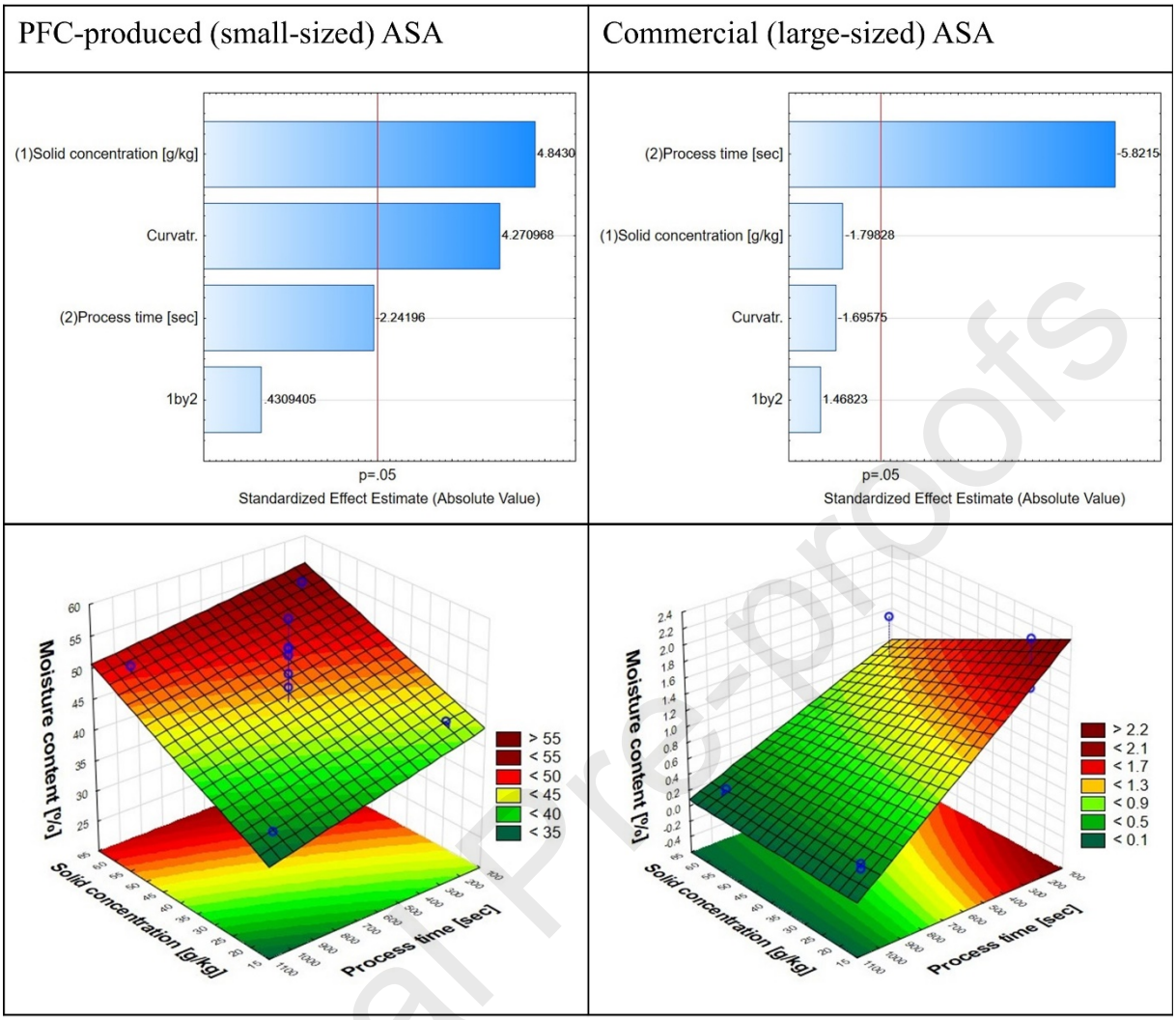

Fig. 7 Pareto charts and Response Surfaces representing the statistical analysis results of filtration experiments processing small- and large-sized ASA.

As proved by the Pareto charts in Fig. 7, the solid concentration and curvature had a statistically significant effect on moisture content in the case of small-sized PFC-produced particles. The significance of curvature means that a quadratic equation is required to accurately describe the behavior of the system, for which further experiments must be carried out. In this study, we did not aim to build the exact mathematical model of the system, so no further experiments were performed. Based on center point PFC-CHBF experiments, it could be stated that by decreasing the crystal size, the residual moisture content within a given setting (up to ±6%) and between parallel samples could also show greater fluctuation. In the case of small particle size ASA, the filtration efficacy could be more sensitive to changes occurring during the process, such as uneven height of filter cake, unevenly spread suspension, and the occurrence of vacuum leaks.

When filtering the large-sized commercial ASA/water suspension, the process time significantly affected φ. By increasing the filtration duration, the φ decreased; this tendency was illustrated by the Response Surface generated by TIBCO Statistica Software (Fig. 7).

In conclusion, the filtration with CHBF is outstandingly robust. The almost completely dried product could be yielded by filtering ethanolic suspensions or large-sized (D_v90: 850 µm) aqueous suspensions. In the case of extreme particle sizes, filtration process parameters affect moisture content. For small

particles (40 μm) with a large specific surface area, solid concentration is influential, while for large particles, process time proved significant.

The integrated continuous crystallization and filtration results are presented in the following sections. Firstly, CHBF was connected to the most commonly utilized continuous crystallizer types, MSMPR crystallizer and PFC. The authors previously studied these crystallization technologies in multiple publications [43,45,48]. Concluding that the crystallization in the MSMPR crystallizer features a longer startup period (min magnitude), while in the PFC, the steady-state operation is reached rapidly in secs. In MSMPR crystallizer, usually larger-sized particles are obtained due to longer RTs, while in PFC, ultrasonication facilitates the crystallization of small and uniform particles.

3.4 Continuous experiments with integrated continuous crystallizer-CHBF system

The CHBF was coupled with the frequently used continuous crystallizers (overflow MSMPR, PFC) to investigate the filtration process in the integrated system and identify the challenges during operation. The continuous crystallization technology aimed to separate the ASA model ingredient from its ethanolic solution using water antisolvent. Afterward, the *in situ*-produced ASA suspensions were filtered using the CHBF.

In this section, we evaluate the MSMPR-CHBF and PFC-CHBF systems operating with similar crystallization parameter settings (SASR: 0.5, room temperature), describing the product characteristics regarding size, CSD, and residual moisture content. Afterward, we studied washing efficacy regarding moisture and impurity content in the case of the smaller crystal-sized PFC-CHBF system.

In Table 9 and Table 10, we detail the sampling location and the time when the samples left the crystallizer and the CHBF filter. During the operation, the effect of the filtration process time was systematically investigated by setting its value at different durations: 200, 600, or 1000 seconds.

Table 9 Sampling locations and times during the experiment with MSMPR-CHBF system.

Sample name	Sampling location	Time, when the sample left the crystallizer*	Time, when the sample left the crystallizer**	Process time set during filtering	Time, when the sample left the filter*
MSMPR-CHBF_1	End of the CHBF	2.7 min	1 RT	200 sec	6.0 min
MSMPR-CHBF_2	End of the CHBF	5.3 min	2 RT	200 sec	8.7 min
MSMPR-CHBF_3	End of the CHBF	10.7 min	4 RT	600 sec	20.7 min
MSMPR-CHBF_4	End of the CHBF	12.0 min	4.5 RT	600 sec	22.0 min
MSMPR-CHBF_5	End of the CHBF	24.0 min	9 RT	1000 sec	40.7 min

MSMPR-CHBF_6	End of the CHBF	25.3 min	9.5 RT	1000 sec	42.0 min
MSMPR_1	MSMPR cryst. overflow tubing	9.9 min	3.7 RT	-	-
MSMPR_2	MSMPR cryst. overflow tubing	25.1 min	9.4 RT	-	-

* time from the start of the experiment in min

** time from the start of the experiment in crystallizer RTs

Table 10 Sampling locations and times during the experiment with PFC-CHBF system.

Sample name	Sampling location	Time, when the sample left the crystallizer*	Time, when the sample left the crystallizer**	Process time set during filtering	Time, when the sample left the filter*
PFC-CHBF_1	End of the CHBF	1.0 min	2 RT	1000 sec	17.7 min
PFC-CHBF_2	End of the CHBF	10.0 min	20 RT	1000 sec	26.7 min
PFC-CHBF_3	End of the CHBF	35.0 min	70 RT	600 sec	45.0 min
PFC-CHBF_4	End of the CHBF	45.0 min	90 RT	600 sec	55.0 min
PFC-CHBF_5	End of the CHBF	65.0 min	130 RT	200 sec	68.3 min
PFC-CHBF_6	End of the CHBF	80.0 min	160 RT	200 sec	83.3 min
PFC_1	End of the PFC	17.5 min	35 RT	-	-

* time from the start of the experiment in min

** time from the start of the experiment in crystallizer RTs

According to Table 9, the product samples named MSMPR_1 and MSMPR-CHBF_3 left the crystallizer at similar timepoints (9.9 min and 10.7 min). The sample MSMPR_1 was collected directly after leaving the MSMPR crystallizer, while MSMPR-CHBF_3 was filtered in the CHBF and collected at the end of the filtration process. A similar sample pair is MSMPR_2 and MSMPR-CHBF_6, as this product left the crystallizer at similar timepoints (25.1 min and 25.3 min). In the case of the PFC-CHBF system, the PFC_1 and PFC-CHBF_2 products were collected at similar timepoints (Table 10).

The product characteristics regarding crystal size, CSD, crystal habit of combining continuous crystallizations with filtration are illustrated in Fig. 8 and Table 11. In Fig. 8, we aimed to present the evolution of D_v values during crystallization and to evaluate the change in particle size that might occur during filtration.

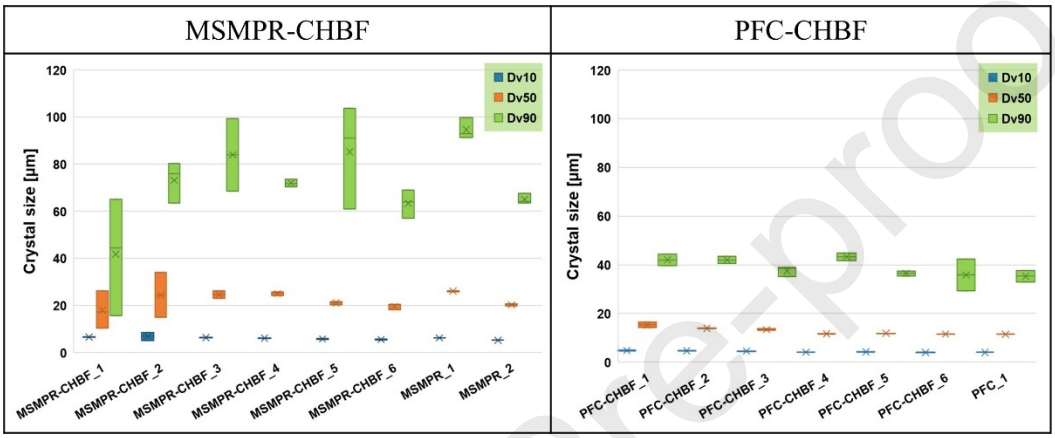

Fig. 8 Evolution of D_v values of the sampled products during continuous operation in the MSMPR-CHBF and PFC-CHBF systems.

Table 11 CSD plots and D_v values [µm] of products yielded from the crystallizers (MSMPR or PFC) or directly from the CHBF.

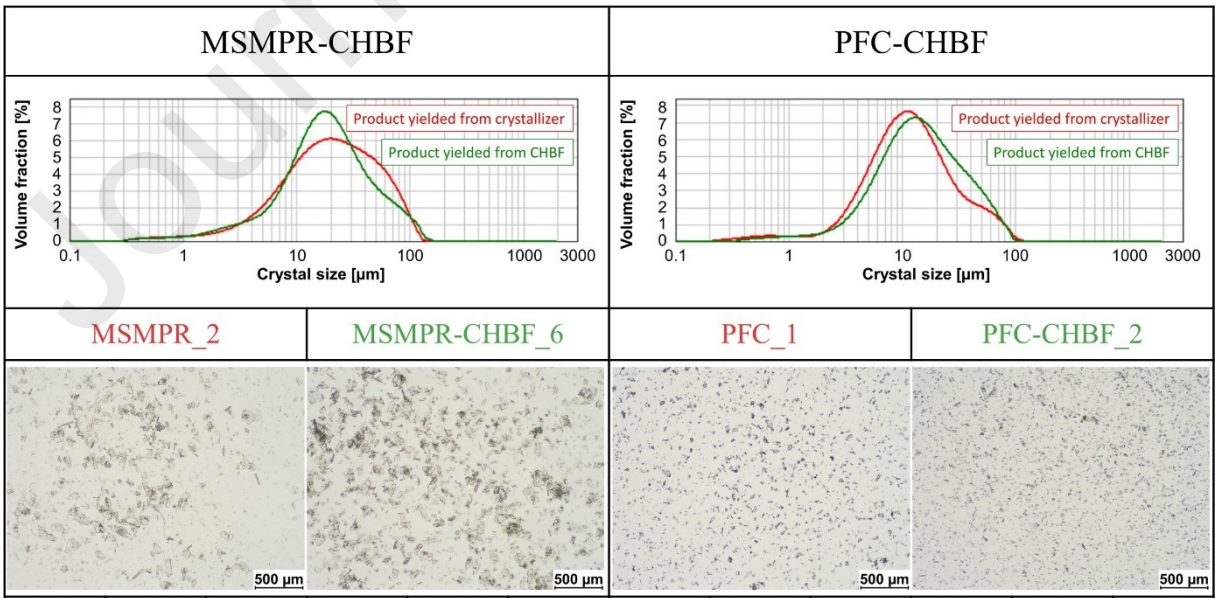

D_v10	D_v50	D_v90	D_v10	D_v50	D_v90	D_v10	D_v50	D_v90	D_v10	D_v50	D_v90
5.7 ± 0.5	23.1 ± 3.2	79.8±16.5	6.1 ± 0.8	22.8 ± 4.5	74.9±14.1	4.1 ± 0.1	11.5 ± 0.0	35.3 ± 3.3	4.4 ± 0.3	13.1 ± 1.4	39.6 ± 4.2

According to Fig. 8 and Table 11, the crystals exiting the crystallizer-filter systems exhibited similar D_v values and crystal habit to the product collected directly from the crystallizers. Specifically, the D_v values of the sample MSMPR-CHBF_6 collected from the MSMPR-CHBF system correlated with the MSMPR_2 product obtained from the MSMPR crystallizer using a glass filter. This suggests that no agglomeration or other processes causing morphological changes occurred in the CHBF. Therefore, we can draw conclusions about the crystallization process by analyzing the characteristics of the product collected from the crystallizer-CHBF system (MSMPR-CHBF). Based on this, in the MSMPR-CHBF system, after a moderate startup phase, the steady state was reached in 2 RT operation (appr. 5 min). The crystals yielded in the MSMPR crystallizer proved to be columnar, larger in size, and featured mainly unimodal CSDs. In contrast, in the PFC, the steady state could be reached faster (in 1 min), and the product characteristics were constant from the first sampling. The PFC product was small and had narrower and unimodal CSD. Our experiences in connection with startup phase, are consistent with what is described in the literature, which states that MSMPR crystallizers typically have a longer startup phase than smaller tubular crystallizers.

The solid concentration and mass flow rate in these experiments depended on the crystallization parameters and were not altered within one experiment. The mass flow rates and RTs in the crystallizers were similar in both the MSMPR-CHBF and PFC-CHBF systems. This similarity facilitated comparable particle sizes in both systems (particle size fell within the same order of magnitude). As a result, the moisture content also fell within the same range, varying between 18% and 25% by adjusting the process time (Table 12). The φ was found to be lower than the φ measured in the similar particle-sized PFC-produced ASA/water system filtered in the standalone CHBF (Section 3.3). In accordance with the literature, the presence of volatile solvents (ethanol) could greatly impact the achievable φ; and thus, facilitate better filtration efficacy.

Table 12 Residual Moisture Content of the Product Manufactured in the MSMPR-CHBF and PFC-CHBF Systems as a Function of Process Time.

	MSMPR-CHBF			**PFC-CHBF**		
Process time [sec]	**200**	**600**	**1000**	**200**	**600**	**1000**
φ [%]	19.6 ± 5.6	24.2 ± 6.5	21.5 ± 13.4	24.8 ± 3.9	22.5 ± 5.8	20.7 ± 7.3

In the case of the PFC-CHBF system, both the washing effect and the RTD of the slurry in the CHBF were investigated. The former is discussed in the following section, while the latter is described in the Supplementary Material of the publication.

Washing in PFC-CHBF

The washing modules in the CHBF enable the introduction of washing liquid during filtration to enhance the purity of the product. Three washing configurations were implemented regarding washing zones: (i) no washing zone, (ii) 1st washing zone, and (iii) both 1st and 2nd washing zones were active. By setting

up these configurations, the influence of washing on residual moisture and salicylic acid (SA) impurity content in the integrated PFC-CHBF system was studied. The process parameters were SASR: 0.5, T: 25°C, and mass flow rate: 35.5 g/min, initial SA impurity content: 5%. The residual moisture and impurity content as a function of the applied washing configurations are summarized in the diagrams of Fig. 9.

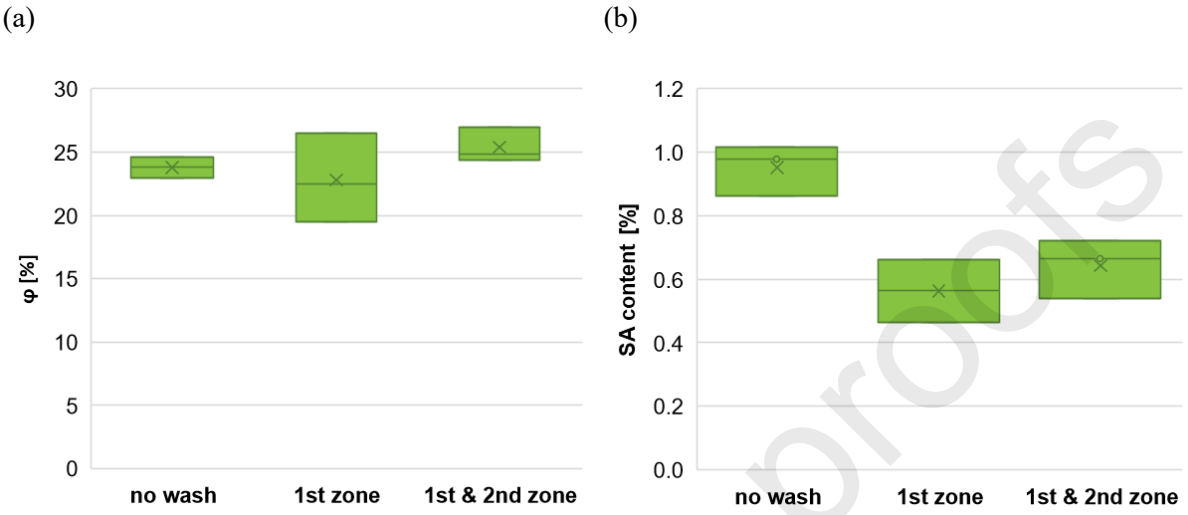

Fig. 9 Residual moisture (a) and SA impurity (b) content of the filtered products as a function of process time during washing experiments.

Fig. 9 (a) shows that the moisture content ranged within a narrow range (46.9-49.4% on average) by changing washing configurations. According to our previous observations, one vacuum zone is enough to withdraw most of the removable mother liquor. In all washing settings, the solids passed about at least two vacuum zone after washing, allowing the mother liquor to be withdrawn. Therefore, there was no significant difference in residual moisture content by implementing washing.

SA, a reagent and byproduct during ASA synthesis, can be the most frequent impurity in an ASA reaction mixture. Therefore, to study the washing efficacy regarding product purity 5% SA was added to the ASA solution; the SA concentration was 8 mg/mL. The SA content in the filtered product was assessed through offline HPLC analysis. According to the results presented in Fig. 9 (b), crystallization in PFC could reduce the SA content to 1%, while washing could further improve the purity to 0.5%. It was found that even one active washing module could significantly reduce the impurity content. In conclusion, the wash performed promisingly, but further experiments are needed to characterize its operational efficiency, which was not the aim of this study.

Some difficulties and challenges regarding the operation of the novel CHBF equipment have been identified. (i) In the narrow environment of slant welding, the filtration efficiency decreases, but this is not affecting the entire filtering process. (ii) The small particle-sized fraction (>10 μm) of the filtered solids could pass the filter clothe and appear in the collected mother liquor; however, it does not cause clogging of the filter medium. (iii) Based on preliminary experiments with the integrated crystallizer-filter system, it is important to avoid crystallization during filtration as precipitated crystals could block the suction troughs. Clogging can be eliminated by washing during the process. In addition, the filtration can be continued with similar efficiency even in case of temporary blockage of some suction troughs. The crystal precipitation during filtration could be effectively avoided by fine-tuning the crystallization process. (iv) The evaluation of washing efficiency requires further experiments.

4. Conclusions

The current study presents a comprehensive overview of the continuously operating horizontal conveyor belt filtration approach applying for filtration of ASA active ingredient and widely used formulation excipients. The never-published CHBF device was tested both in standalone mode and in integrated crystallizer-filter systems. The residual moisture content was measured by varying filtration process parameters (process time, mass flow rate, solid concentration) and suspension characteristics (solvent, crystal size). The CHBF was found to be robust by processing aqueous systems at almost every investigated particle size range, as it could operate with similar efficacy by varying mass flow rates, solid concentration, and process time. Among these, processing the slurry of small particles (D_v90: 42 μm) was less effective, and a product with 37-55% residual moisture content was yielded. In contrast, larger (D_v90: 850 μm) particles could almost completely dry even from their aqueous suspension at the end of the filtration. The CHBF performed outstanding in processing slurries of volatile solvents, as the residual moisture content could be reduced to 0.3-1.4%.

In the integrated crystallizer-filter system, the filter was operated steadily without altering the characteristics of the MSMPR- or PFC-produced particles. Due to the ethanol content in the crystallized suspension, the residual moisture content could be reduced to 20%. Introducing the washing liquid during filtration could even enhance the purity of the small-sized product while the filtration efficacy is maintained at the same level.

Overall, the tested lab-scale CHBF device proved to be effective and robust in separating various particle-sized solids from their aqueous and ethanolic suspensions. It could be integrated with lab-scale continuous crystallizations; furthermore, experiments with increased workload suggest that the equipment could efficiently meet higher capacity requirements. This makes the CHBF exceptionally potent for continuous pharmaceutical filtration.

ACKNOWLEDGMENT

The authors are grateful to the H-ION Chemistry Team for providing the filter equipment and supporting this work. This work was financially supported by the National Research Development and Innovation Office of Hungary (FK-143019, PD-142970). Project no. RRF-2.3.1-21-2022-00015 has been implemented with the support provided by the European Union. Brigitta Nagy is thankful for the János Bolyai Research Scholarship of the Hungarian Academy of Sciences. The research was also supported by the ÚNKP-22-4-I-BME-257 and ÚNKP-23-5-BME-443 New National Excellence Program of the Ministry for Culture and Innovation from the source of the National Research, Development and Innovation Fund.

REFERENCES

[1] FDA, Pharmaceutical CGMPs for the 21s Century - A risk-based approach, (2004) 32. http://www.fda.gov/Drugs/DevelopmentApprovalProcess/Manufacturing/QuestionsandAnswersonCurrentGoodManufacturingPracticescGMPforDrugs/UCM071836.

[2] S. Chatterjee, FDA Perspective on Continuous Manufacturing, IFPAC Annu. Meet. (2012) 21. https://www.fda.gov/downloads/aboutfda/centersoffices/officeofmedicalproductsandtobacco/cder/ucm341197.pdf.

[3] J. Kossik, Operation of a Disposable Rotary Drum Filter, Present. AIChE Annu. Meet. , Pharm.

Biotechnol. Pilot Plants. (2001).

[4] J.M. Kossik, J.F. Delys, DISPOSABLE ROTARY DRUM FILTER, 2002.

[5] J. Kossik, Small scale continuous cake filtration using the disposable rotary drum filter, Filtr. Sep. 40 (2003) 26–27. https://doi.org/10.1016/S0015-1882(03)00926-1.

[6] J. Gursch, R. Hohl, G. Toschkoff, D. Dujmovic, J. Brozio, M. Krumme, N. Rasenack, J. Khinast, Continuous Processing of Active Pharmaceutical Ingredients Suspensions via Dynamic Cross-Flow Filtration, J. Pharm. Sci. 104 (2015) 3481–3489. https://doi.org/10.1002/jps.24562.

[7] J. Gursch, R. Hohl, D. Dujmovic, J. Brozio, M. Krumme, N. Rasenack, J. Khinast, Dynamic cross-flow filtration: Enhanced continuous small-scale solid-liquid separation, Drug Dev. Ind. Pharm. 42 (2016) 977–984. https://doi.org/10.3109/03639045.2015.1100200.

[8] S. Mascia, P.L. Heider, H. Zhang, R. Lakerveld, B. Benyahia, P.I. Barton, R.D. Braatz, C.L. Cooney, J.M.B. Evans, T.F. Jamison, K.F. Jensen, A.S. Myerson, B.L. Trout, End-to-end continuous manufacturing of pharmaceuticals: Integrated synthesis, purification, and final dosage formation, Angew. Chemie - Int. Ed. 125 (2013) 12585–12589. https://doi.org/10.1002/anie.201305429.

[9] C.J. Testa, C. Hu, K. Shvedova, W. Wu, R. Sayin, F. Casati, B.S. Halkude, P. Hermant, D.E. Shen, A. Ramnath, Q. Su, S.C. Born, B. Takizawa, S. Chattopadhyay, T.F. O'Connor, X. Yang, S. Ramanujam, S. Mascia, Design and Commercialization of an End-to-End Continuous Pharmaceutical Production Process: A Pilot Plant Case Study, Org. Process Res. Dev. 24 (2020) 2874–2889. https://doi.org/10.1021/acs.oprd.0c00383.

[10] C. Hu, C.J. Testa, S.C. Born, W. Wu, K. Shvedova, R. Sayin, B.S. Halkude, F. Casati, A. Ramnath, P. Hermant, B. Takizawa, T.F. O'Connor, X. Yang, S. Ramanujam, S. Mascia, E-factor analysis of a pilot plant for end-to-end integrated continuous manufacturing (ICM) of pharmaceuticals, Green Chem. 22 (2020) 4350–4356. https://doi.org/10.1039/d0gc01397h.

[11] C. Hu, C.J. Testa, W. Wu, K. Shvedova, D.E. Shen, R. Sayin, B.S. Halkude, F. Casati, P. Hermant, A. Ramnath, S.C. Born, B. Takizawa, T.F. O'Connor, X. Yang, S. Ramanujam, S. Mascia, An automated modular assembly line for drugs in a miniaturized plant, Chem. Commun. 56 (2020) 1026–1029. https://doi.org/10.1039/c9cc06945c.

[12] S.C. Born, J. V. Dittrich, B.T. Takizawa, S. Mascia, Continuous Rotary Plate Filter and Methods of Use Thereof, WO 2017/136779 Al, 2017.

[13] W. Wu, R. Sayin, K. Shvedova, S.C. Born, C.J. Testa, S.S. Yeole, A.S. Censullo, A.K. Srivastava, A. Ramnath, C. Hu, B. Takizawa, T.F. O'Connor, X.B. Yang, S. Ramanujam, S. Mascia, A Continuous Rotary Filtration for the Separation and Purification of an Active Pharmaceutical Ingredient, Org. Process Res. Dev. (2023). https://doi.org/10.1021/acs.oprd.3c00263.

[14] S. Ottoboni, C.J. Price, C. Steven, E. Meehan, A. Barton, P. Firth, A. Mitchell, F. Tahir, Development of a Novel Continuous Filtration Unit for Pharmaceutical Process Development and Manufacturing, J. Pharm. Sci. 108 (2019) 372–381. https://doi.org/10.1016/j.xphs.2018.07.005.

[15] A.W. Barton, Filtration Apparatus, WO 2015/033117 A1, 2015.

[16] D. Acevedo, R. Peña, Y. Yang, A. Barton, P. Firth, Z.K. Nagy, Evaluation of mixed suspension mixed product removal crystallization processes coupled with a continuous filtration system, Chem. Eng. Process. Process Intensif. 108 (2016) 212–219.

https://doi.org/10.1016/j.cep.2016.08.006.

[17] S. Ottoboni, M. Shahid, C. Steven, S. Coleman, E. Meehan, A. Barton, P. Firth, R. Sutherland, C.J. Price, Developing a Batch Isolation Procedure and Running It in an Automated Semicontinuous Unit: AWL CFD25 Case Study, Org. Process Res. Dev. 24 (2020) 520–539. https://doi.org/10.1021/acs.oprd.9b00512.

[18] Y.C. Liu, A. Domokos, S. Coleman, P. Firth, Z.K. Nagy, Development of Continuous Filtration in a Novel Continuous Filtration Carousel Integrated with Continuous Crystallization, Org. Process Res. Dev. 23 (2019) 2655–2665. https://doi.org/10.1021/acs.oprd.9b00342.

[19] A. Domokos, B. Nagy, M. Gyürkés, A. Farkas, K. Tacsi, H. Pataki, Y. Claire Liu, A. Balogh, P. Firth, B. Szilágyi, G. Marosi, Z.K. Nagy, Z. Kristóf Nagy, End-to-End Continuous Manufacturing of Conventional Compressed Tablets: from Flow Synthesis to Tableting through Integrated Crystallization and Filtration, Int. J. Pharm. (2020) 119297. https://doi.org/10.1016/j.ijpharm.2020.119297.

[20] G. Schembecker, K. Wohlgemuth, C.M. Steenweg, Rotating-screw drying reactor, US 20230063353 A1, 2020.

[21] C. Steenweg, A.I. Seifert, N. Böttger, K. Wohlgemuth, Process Intensification Enabling Continuous Manufacturing Processes Using Modular Continuous Vacuum Screw Filter, Org. Process Res. Dev. 25 (2021) 2525–2536. https://doi.org/10.1021/acs.oprd.1c00294.

[22] C. Steenweg, J. Habicht, K. Wohlgemuth, Continuous Isolation of Particles with Varying Aspect Ratios up to Thin Needles Achieving Free-Flowing Products, Crystals. 12 (2022). https://doi.org/10.3390/cryst12020137.

[23] C. Steenweg, A.C. Kufner, J. Habicht, K. Wohlgemuth, Towards continuous primary manufacturing processes— particle design through combined crystallization and particle isolation, Processes. 9 (2021). https://doi.org/10.3390/pr9122187.

[24] C. Steenweg, A.I. Seifert, G. Schembecker, K. Wohlgemuth, Characterization of a Modular Continuous Vacuum Screw Filter for Small-Scale Solid-Liquid Separation of Suspensions, Org. Process Res. Dev. 25 (2021) 926–940. https://doi.org/10.1021/acs.oprd.0c00550.

[25] J. Sonnenschein, M. Hermes, S. Höving, N. Kockmann, K. Wohlgemuth, Population balance modeling of unstirred cooling crystallization on an integrated belt filter, Comput. Chem. Eng. 167 (2022) 108024. https://doi.org/10.1016/j.compchemeng.2022.108024.

[26] T. Dobler, B. Radel, M. Gleiss, H. Nirschl, Quasi-Continuous Production and Separation of Lysozyme Crystals on an Integrated Laboratory Plant, Crystals. 11 (2021) 713.

[27] T. Dobler, S. Buchheiser, M. Gleiß, H. Nirschl, Development and commissioning of a small-scale, modular and integrated plant for the quasi-continuous production of crystalline particles, Processes. 9 (2021) 663. https://doi.org/10.3390/pr9040663.

[28] T. Dobler, S. Höving, C. Dreiser, M. Gleiß, M. Gröschen, A. Henkel, M. Hörne, M. Schäfer, J. Sonnenschein, G. Wiese, K. Wohlgemuth, N. Kockmann, H. Nirschl, From Lab to Pilot Scale: Commissioning of an Integrated Device for the Generation of Crystals, Chem. Eng. Technol. 46 (2023) 1511–1520. https://doi.org/10.1002/ceat.202200616.

[29] S. Höving, P. Bolien, P. Siebers, N. Kockmann, Simplified Approach to Characterize the Cooling Crystallization in a Modular Mini-Plant, Crystals. 13 (2023). https://doi.org/10.3390/cryst13010147.

[30] S. Höving, B. Oldach, N. Kockmann, Cooling Crystallization with Complex Temperature Profiles on a Quasi-Continuous and Modular Plant, Processes. 10 (2022). https://doi.org/10.3390/pr10061047.

[31] S. Höving, T. Schmidt, M. Peters, H. Lapainis, N. Kockmann, Small-Scale Solids Production Plant with Cooling Crystallization, Washing, and Drying in a Modular, Continuous Plant, Processes. 11 (2023) 2457.

[32] Y. Yang, Z.K. Nagy, Combined cooling and antisolvent crystallization in continuous mixed suspension, mixed product removal cascade crystallizers: Steady-state and startup optimization, Ind. Eng. Chem. Res. 54 (2015) 5673–5682. https://doi.org/10.1021/ie5034254.

[33] S.Y. Wong, A.P. Tatusko, B.L. Trout, A.S. Myerson, Development of continuous crystallization processes using a single-stage mixed-suspension, mixed-product removal crystallizer with recycle, Cryst. Growth Des. 12 (2012) 5701–5707. https://doi.org/10.1021/cg301221q.

[34] R.J.P. Eder, S. Radl, E. Schmitt, S. Innerhofer, M. Maier, H. Gruber-Woelfler, J.G. Khinast, Continuously seeded, continuously operated tubular crystallizer for the production of active pharmaceutical ingredients, Cryst. Growth Des. 10 (2010) 2247–2257. https://doi.org/10.1021/cg9015788.

[35] M.N. Hussain, J. Jordens, J.J. John, L. Braeken, T. Van Gerven, Enhancing pharmaceutical crystallization in a flow crystallizer with ultrasound: Anti-solvent crystallization, Ultrason. Sonochem. 59 (2019) 104743. https://doi.org/10.1016/j.ultsonch.2019.104743.

[36] M.O. Besenhard, P. Neugebauer, O. Scheibelhofer, J.G. Khinast, Crystal engineering in continuous plug-flow crystallizers, Cryst. Growth Des. 17 (2017) 6432–6444. https://doi.org/10.1021/acs.cgd.7b01096.

[37] M. Huttunen, L. Nygren, T. Kinnarinen, B. Ekberg, T. Lindh, J. Ahola, V. Karvonen, A. Häkkinen, Specific energy consumption of vacuum filtration: Experimental evaluation using a pilot-scale horizontal belt filter, Dry. Technol. 38 (2019) 460–475. https://doi.org/10.1080/07373937.2019.1581214.

[38] D. Gehrmann, N. Schweigler, DEVICE FOR CONTINUOUS FILTRATION AND DRYING OF A SOLID SUSPENSION, US005527458A, 1996.

[39] L. Hohmann, L. Löbnitz, C. Menke, B. Santhirakumaran, P. Stier, F. Stenger, F. Dufour, G. Wiese, S. zur zur Horst-Meyer, B. Kusserow, W. Zang, H. Nirschl, N. Kockmann, Continuous Downstream Processing of Amino Acids in a Modular Miniplant, Chem. Eng. Technol. 41 (2018) 1152–1164. https://doi.org/10.1002/ceat.201700657.

[40] M. Huttunen, L. Nygren, T. Kinnarinen, B. Ekberg, T. Lindh, V. Karvonen, J. Ahola, A. Häkkinen, Real-time monitoring of the moisture content of filter cakes in vacuum filters by a novel soft sensor, Sep. Purif. Technol. 223 (2019) 282–291. https://doi.org/10.1016/j.seppur.2019.03.091.

[41] BHS-SONTHOFEN, BF Indexing Belt Filter, (2012).

[42] J. Garrick, Process Design Strategy: The Advantages of Continuous Filtration for Pharmaceutical Manufacturing, InformEx. (2015). https://bhs-filtration.com/process-design-strategy-the-advantages-of-continuous-filtration-for-pharmaceutical-manufacturing/.

[43] K. Tacsi, G. Stoffán, É. Pusztai, B. Nagy, A. Domokos, B. Szilágyi, Z.K. Nagy, G. Marosi, H. Pataki, Implementation of sonicated continuous plug flow crystallization technology for processing of acetylsalicylic acid reaction mixture, Powder Technol. 400 (2022) 117255.

https://doi.org/10.1016/j.powtec.2022.117255.

[44] A.H. Ostadhashem, K. Peyvandi, Measurement solubility of Acetylsalicylic Acid in water and alcohols, Int. Pharm. Acta. 3 (2020) 3e11:1-7. https://journals.sbmu.ac.ir/acta/article/view/32231.

[45] K. Tacsi, A. Joo, E. Pusztai, A. Domokos, Z.K. Nagy, G. Marosi, H. Pataki, Development of a Triple Impinging Jet Mixer for Continuous Antisolvent Crystallization of Acetylsalicylic Acid Reaction Mixture, Chem. Eng. Process. - Process Intensif. (2021) 108446. https://doi.org/10.1016/j.cep.2021.108446.

[46] A. Balogh, A. Domokos, B. Farkas, A. Farkas, Z. Rapi, D. Kiss, Z. Nyiri, Z. Eke, G. Szarka, R. Örkényi, B. Mátravölgyi, F. Faigl, G. Marosi, Z.K. Nagy, Continuous end-to-end production of solid drug dosage forms: Coupling flow synthesis and formulation by electrospinning, Chem. Eng. J. 350 (2018) 290–299. https://doi.org/10.1016/j.cej.2018.05.188.

[47] J. Fogel, P. Epstein, P. Chen, Simultaneous high-performance liquid chromatography assay of acetylsalicylic acid and salicylic acid in film-coated aspirin tablets, J. Chromatogr. A. 317 (1984) 507–511. https://doi.org/10.1016/S0021-9673(01)91690-5.

[48] K. Tacsi, H. Pataki, A. Domokos, B. Nagy, I. Csontos, I. Markovits, F. Farkas, Z.K. Nagy, G. Marosi, Direct Processing of a Flow Reaction Mixture Using Continuous Mixed Suspension Mixed Product Removal Crystallizer, Cryst. Growth Des. 20 (2020) 4433–4442. https://doi.org/10.1021/acs.cgd.0c00252.

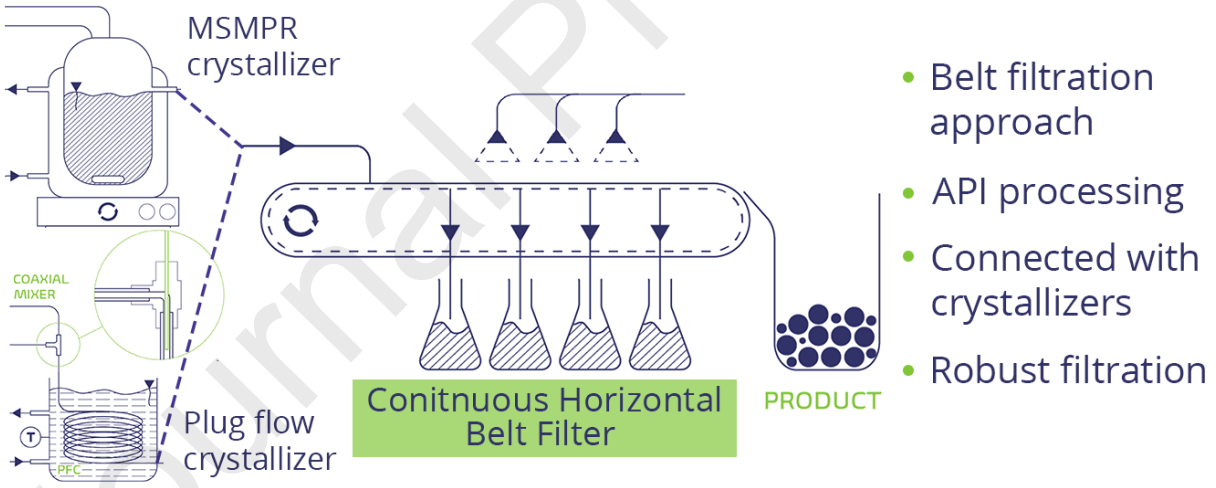

Declaration of interests

☒ The authors declare that they have no known competing financial interests or personal relationships that could have appeared to influence the work reported in this paper.

☐ The authors declare the following financial interests/personal relationships which may be considered as potential competing interests: